Icosapent ethyl reduces arterial thrombosis by inhibition of cyclooxygenase-1 induced platelet reactivity

Philipp Mourikis[1*], Marcel Benkhoff[1*], Laura Wildeis[1*], Maike Barcik[1], Carolin Helten[1], Cristina Coman[2], Fiorella A. Solari[3], Daniel Krahn[3], Lisa Dannenberg[1], Samantha Ahlbrecht[1], Dorothee Zikeli[1], Amelie Utz[1], Kajetan Trojovsky[1], Hannah Richter[1], Gabrielle Al Kassis[1], René M'Pembele[4], Saif Zako[1], Tim Huckenbeck[1], Sofia Bauer[1], Danny Schmitz[1], Susanne Pfeiler[1], Norbert Gerdes[1], Christof Dücker[5], Joachim Pircher[6], Zhang Zhe[6, 18, 19], Manuela Thienel[6], Qurrat Ul Ain[6], Petra Keul[7], Nicholas Kirkby[8], Dennis Sohn[9], Wilfried Budach[9], Thomas Hohlfeld[10], Karsten Schrör[10], Bodo Levkau[7], Tobias Zeus[1], Steven H.L. Verhelst[3,11], Robert Ahrends[2], Albert Sickmann[3, 12, 13], Jane Mitchell[8], Samia Mora[14, 15], JoAnn E. Manson[14,16], Deepak L Bhatt[17], Ulf Landmesser[18], Steffen Massberg[6], Malte Kelm[1], Tobias Petzold[18, 19, 20*], Amin Polzin[1*]

[1]Division of Cardiology, Pulmonology, and Vascular Medicine, Medical Faculty, Heinrich Heine University Medical Center Dusseldorf, 40225 Dusseldorf, Germany

[2]Institute of Analytical Chemistry, University of Vienna, 1090 Vienna, Austria

[3]Leibniz-Institut für Analytische Wissenschaften – ISAS – e.V., 44227 Dortmund, Germany

[4]Department of Anesthesiology, Medical Faculty, Heinrich Heine University Medical Center Dusseldorf, 40225 Dusseldorf, Germany

[5]Institute for Clinical Pharmacology, University Medical Center, Georg-August University, Göttingen, 37027 Göttingen, Germany

[6]Medizinische Klinik und Poliklinik I, Klinikum der Universität München, Ludwig-Maximilians-Universität München, 80539 München, Deutschland

[7]Institute for Molecular Medicine III, Heinrich Heine University Dusseldorf, 40225 Dusseldorf Germany

[8]Faculty of Medicine National Heart & Lung Institute, Imperial College London, SW7 2BX London, United Kingdom

[9]Laboratory of Molecular Radiooncology, Clinic and Policlinic for Radiation Therapy and Radiooncology, Medical Faculty of the Heinrich Heine University, 40225 Dusseldorf, Germany

[10]Institute for Pharmacology and Clinical Pharmacology, Medical Faculty, Heinrich Heine University, 40225 Dusseldorf, Germany

[11]Laboratory of Chemical Biology, Department of Cellular and Molecular Medicine, KU Leuven, 3000 Leuven, Belgium

[12]Medizinische Fakultät, Medizinische Proteom-Center, Ruhr-Universität Bochum, 44801 Bochum, Germany.

[13]Department of Chemistry, College of Physical Sciences, University of Aberdeen, Aberdeen AB24 3FX, UK.

[14]Division of Preventive Medicine, Department of Medicine, Brigham and Women's Hospital and Harvard Medical School, 02115 Boston, Massachusetts

[15]Cardiovascular Division, Department of Medicine, Brigham and Women's Hospital and Harvard Medical School, 02115 Boston, Massachusetts

[16]Department of Epidemiology, Harvard T.H. Chan School of Public Health, 02115 Boston, Massachusetts

[17]Mount Sinai Heart, Icahn School of Medicine at Mount Sinai Health System, New York, 10029 NY, USA

[18]Deutsches Herzzentrum der Charité (DHZC) University Hospital Berlin, Department of Cardiology, Angiology and Intensive Care Medicine, Campus Benjamin Franklin, 12203 Berlin, Germany

[19]DZHK (German Centre for Cardiovascular Research), Partner site Berlin 12203, Germany

[20]Friede Springer - Centre of Cardiovascular Prevention @ Charité, Charité – University Medicine Berlin, 12203 Berlin, Germany

*authors contributed equally

Corresponding author:
Prof. Dr. med. A. Polzin
Moorenstraße 5, 40225 Düsseldorf
Klinik für Kardiologie, Pneumologie und Angiologie
Universitätsklinikum Düsseldorf
Fax: 0049-211-81-18812
Phone: 0049-211-81-18800
amin.polzin@med.uni-duesseldorf.de

OVERLINE:

One-sentence summary: Dose-dependent platelet inhibition by icosapent ethyl contributes to beneficial effects of polyunsaturated omega-3 fatty acids.

Editor's summary:

Abstract:

Large, randomized trials testing omega-3 polyunsaturated fatty acid (ω-3 PUFA) supplementation to reduce cardiovascular events have reported contradictory results. Interpretation of these trials is challenging, as different dosages and formulations of ω-3 PUFA were tested. Furthermore, the exact mechanisms for the reduction in cardiovascular events are unclear. In this study, we investigated the effects of ω-3 PUFA on platelet adhesion, degranulation and aggregation in vitro and in patients with cardiovascular disease using different formulations of ω-3 PUFA. We also investigated the effects of ω-3 PUFA in rodent models of arterial thrombosis and tail bleeding assay (including cyclooxygenase-1 deficient animals), and in photoaffinity-labelling and in silico docking experiments to confirm binding of eicosapentaenoic acid (EPA) to platelet cyclooxygenase-1 (COX-1). The ω-3 PUFA EPA dose-dependently reduced platelet adhesion, degranulation, and aggregation in vitro. Moreover, arterial thrombus formation in wildtype mice was inhibited by oral EPA-administration before thrombus formation. Photoaffinity-labelling and in silico docking analyses suggested a direct, competitive interaction of EPA and arachidonic acid at the level of COX-1. COX-1-dependency of EPA's inhibitory effects was confirmed by platelet specific COX-1 deficient animals that had no reduction of thrombus burden by EPA. In patients with cardiovascular disease, switching from 2 grams EPA twice daily to 1 gram docosahexaenoic acid (460 mg EPA, 380 mg DHA) once daily, completely blunted the platelet inhibition achieved by EPA. Our results may partially explain contradictory results with different ω-3 PUFA formulations in clinical trials.

Introduction

Omega-3 polyunsaturated fatty acid (ω-3 PUFA) supplementation to prevent cardiovascular events remains a matter of debate. Initially, diet with high amounts of fish oil rich in ω-3 PUFA was shown to be associated with a reduction in cardiovascular disease in a Greenlandic population which was the first study to show this association back in the 1970s(*1*). Eicosapentaenoic acid (EPA) is an ω-3 PUFA especially synthesized in marine fish.

Recent randomized controlled trials investigating ω-3-PUFA-supplementation presented inconsistent results. In ASCEND, patients with diabetes but without atherosclerotic cardiovascular disease received 1 gram (g) ω-3 PUFA per day or olive oil as matching placebo. In this trial, the ω-3 PUFA did not provide a benefit over the placebo regarding serious vascular events like myocardial infarction.(*2*) VITAL tested 640 mg EPA and 380 mg docosahexaenoic acid (DHA) per day in a context of primary prevention resulting in no reduction of cardiovascular events in comparison to placebo(*3*). The STRENGTH-trial evaluated the effect of 4 g ω-3 PUFA per day combined of EPA and DHA in statin-treated patients with high cardiovascular risk against corn oil as a placebo which again resulted in no relevant reduction of cardiovascular events(*4*). However, the REDUCE-IT trial revealed cardiac risk reduction using icosapent ethyl (IPE), the ethyl ester of EPA, in a dose of 2 g twice daily. In the REDUCE-IT trial, a cohort of patients with high cardiovascular risk and high triglycerides were included(*5*). Along this line, the Japanese JELIS-trial reported reduction of cardiovascular events as well upon administration of 1.8 g EPA per day in patients with hypercholesterinaemia(*6*). Moreover bleeding events in JELIS and REDUCE-IT were higher in patients receiving ω-3 PUFA- supplementation with EPA which may indicate an antithrombotic effect of EPA in these trials. In summary, the underlying mechanisms of these conflicting clinical results on ω-3 PUFA in cardiovascular disease remain elusive.

After intake, IPE is converted by gut lipases into EPA which is absorbed as active metabolite into the circulation(*7*). EPA consists of 20 carbon atoms and 5 double bonds (C20:5) and is structurally close to arachidonic acid (AA) a ω-6 PUFA with 20 carbon atoms, but 4 double

bonds (C20:4) a main regulator of platelet function. Platelet cyclooxygenase-1 (COX-1) is the predominant AA metabolizing enzyme resulting in the production of thromboxane-A2 (TXA2) which acts as platelet released agonist (*8*), augmenting platelet activation and thrombus formation (*9*). Clinically, COX-1 inhibition by aspirin is frequently used to reduce TXA2 production, platelet activation and thrombosis while fostering bleeding events. Beyond this, EPAs derived metabolites may impact platelet function. Endothelial COX-1 metabolizes EPA into prostaglandin I3 (PGI3) attenuating platelet function in vitro(*10*). In contrast the role of EPA-derived oxylipins including 5-lipoxygenase (LOX) derived 5- hydroxy-eicosapentaenoic acid (5-HEPE), 12-LOX metabolite 12- HEPE, CYP450 metabolized 20-HEPE or non-enzymatic oxidized 18-hydroxy-eicosapentaenoic acid remains elusive (*11*).

Given the structural similarities between EPA and AA, it can be hypothesized that IPE-supplementation may lead to a substrate competition on the level of COX-1 potentially interfering with AA-induced platelet activation and platelet driven thrombosis.

Results

IPE reduces arterial thrombosis in vivo

First, we investigated the impact of oral long term (14 days) IPE-supplementation on arterial thrombus formation in a murine $FeCl_3$-carotid injury model by intravital microscopy. Upon IPE-treatment we observed a delayed occlusion (control: 9.4 min ± 1.6 min vs. IPE: 60 min ± 0 $p<0.0001$), followed by an earlier reperfusion in IPE-treated mice. In addition, maximal thrombus sizes were decreased after IPE-treatment (Fig. 1A and S1A). Subsequently, histological analysis of thrombi revealed a reduced coverage of CD41 and fibrinogen accompanied by a less compact thrombus structure (Fig. 1B and S1B). A bleeding assay revealed increased blood-loss and elevated bleeding time after IPE-intake in comparison to corn oil as placebo (Fig. 1C).

Next, we evaluated the influence of intravenous EPA on arterial thrombus formation in comparison to placebo. We injected EPA emulsion in increasing concentrations intravenous into mice and performed in vitro arterial thrombus formation. We found that 10 % and 20 % emulsions of EPA resulted in an inhibition of arterial thrombus formation and displayed significantly higher time to first occlusion ($p<0.0001$, fig. S2A). Moreover, even a 5 % EPA emulsion resulted in a numerically, but not statistically significant, shorter duration of first occlusion (fig. S2B).

EPA reduces platelet aggregation, adhesion, activation, degranulation and calcium signaling in vitro

To further investigate the underlying mechanism driving the observed antithrombotic effects under IPE treatment, we investigated the impact of EPA, the bioactive metabolite of IPE, on human platelet function in vitro. First, we studied EPA's effect on in vitro thrombus formation under arterial flow on collagen and human atherosclerotic plaque material. EPA treatment reduced platelet adhesion (control: 29.6 % ± 20.7 % vs. EPA 1000 µM: 6.8 % ± 3.7 %, $p=0.0367$) and thrombus burden on plaque material (Fig. 2A and B). In addition, we found

reduced platelet aggregation with EPA upon stimulation with plaque material in comparison to control (fig. S3A).

Light transmission aggregometry (LTA) and whole blood impedance aggregometry were used to evaluate EPA's in vitro effects on platelet aggregation. We revealed a concentration-dependent inhibition of EPA on both aggregation responses in platelet rich plasma (control: 83.0 % ± 6.3 % vs. EPA 1000 µM: 20.9 % ± 36.3 %, p=0.0099) and whole blood in comparison to vehicle treated control blood (Fig. 2C and D, fig. S3B and C). EPA reduced ATP release as marker for dense granule release in comparison to the control (Fig. 2E). Furthermore, alpha-granule release after activation was inhibited by EPA assessed by p-selectin-expression when compared to the control (Fig. 2F). Moreover, EPA reduced platelet activation on single cell level in a concentration-dependent manner in comparison to the control after stimulation with AA, ADP, and collagen quantified by CD41/61, CD40, CD40L, and PAC-1-expression (fig. S3D). In addition, AA-induced intracellular Ca^{2+}-concentration was impaired by EPA preincubation (Fig. 2G). Moreover, we measured TXB2 as a stable metabolite of TXA2 after in vitro incubation of platelets with increasing concentrations of EPA. We found that EPA inhibited AA-induced TXB2-production in vitro in comparison to the control (Fig. 2H).

EPA treatment alters intracellular platelet signaling in vitro

To elucidate the molecular basis of EPA treatment on platelet physiology we performed phosphoproteomics analysis with human platelets. EPA treatment resulted in modulation of intracellular protein phosphorylation and abolished AA-induced protein phosphorylation (Fig. 3A and B). Adenylate cyclase type 6 was increased due to AA-treatment in comparison to the vehicle treated control. This effect was reduced by additional EPA treatment. Next, we investigated diacylglycerol kinase gamma which has an important role in calcium release in platelets. Again, AA-treatment led to an increasement, and EPA-treatment abolished this in comparison to the control. Third, we observed a similar pattern for inositol 1, 4, 5-triphosphate receptor associated 1 which is also involved in the calcium release in platelets. AA-treatment

led to an increase in comparison to the control and an additional EPA-treatment reduced the AA-induced increase (Fig. 3C).

EPA and AA interact competitive at platelet COX-1

To address whether the observed alteration in platelet function are due to a competition of AA and EPA for COX-1 binding, we designed a covalent chemical probe suitable for photoaffinity labeling on recombinant human COX-1. Photo crosslinking was carried out under UV irradiation (365nm) at room temperature. The fluorescently labeled protein was detected by in-gel scanning confirming platelet COX-1 as target of EPA in vitro. Fluorescence intensity was higher with the probe (EPA) in comparison to the DMSO-control. (Fig. 4A).

Next, we aimed to identify EPA's molecular mode of action. We hypothesized direct interaction between EPA and COX-1. Virtual docking suggested a position with maximal affinity for EPA in COX-1 with the carboxylic acid group of EPA oriented toward one of two hydrophilic regions close to the channel. In this configuration, the aliphatic chain of EPA blocks the hydrophobic channel pointing towards the serine530 and tyrosine385 of platelet COX-1. Comparison of docking of AA into COX-1 with its position in a crystal structure revealed good overlap of the docked structure.(Fig. 4B). We then docked EPA into the COX-1 structure and found that the position and affinity of nine modes was similar to AA (Fig. 4B).

To illustrate a COX-1-dependent antiplatelet effect of EPA, we examined platelet function under pharmacological COX-1 blockade using acetylsalicylic acid (ASA). EPA showed no additional effect on platelet adhesion and AA-induced aggregation after COX-1 blockade with ASA in vitro (Fig. 4C and D). Vice versa, we tested the reversibility of EPA-effects on COX-1 using increasing AA concentrations. We found that COX-1 inhibition by EPA was overcome by increasing concentrations of AA (0.5 mM AA: 25.8 % ± 31.4 % vs. 1 mM AA: 78.3 % ± 4.7 %, p=0.0111; 1 mM AA vs. 2 mM AA: 65.9 % ± 20.9 %, p=0.0397). In contrast, ASA pretreatment was not reversible and increasing AA-concentrations did not overcome platelet inhibition by ASA (Fig. 4E). To rule out that the mechanism of platelet inhibition is dependent on reduction

of triglycerides, we analyzed platelet function in 370 patients treated with ASA, revealing no correlation between AA-induced maximum of aggregation (MoA) and triglyceride-concentrations (Fig. 4F). Patients treated with ASA were 67.8 ± 12.3 years old, 60.8 % were male and 23.3 % were obese. Further characteristics are presented in table S1. To investigate if changed membrane composition contributed to IPE's antiplatelet effects, we measured membrane lipid release during platelet activation. The AA/EPA ratio during platelet activation did not differ after IPE supplementation in comparison to baseline (Fig. 4G and H). This suggested that the mechanism of reduced platelet reactivity in patients treated with IPE treated did not require changes in platelet membrane composition. To further investigate the interaction between COX-1 and EPA, we performed a COX-inhibition assay in vitro with recombinant COX-1. Relative COX-1-inhibition increased with higher concentrations of EPA in comparison to the control without EPA (Fig. 4I).

Pharmacological COX-1-blockade and platelet-specific COX-1 deficiency abolish IPE's antiplatelet effects in vivo

We next investigated the effects of IPE/EPA on thrombus formation in vivo by using two animal models. First, we pretreated wildtype mice with ASA orally to inhibit COX-1 enzymatic activity. To test whether IPE reduced platelet responses and arterial thrombus formation in vivo, we visualized $FeCl_3$-induced thrombus formation in these mice. IPE pretreatment did not show any additional effect on thrombus formation in comparison to ASA-treated mice. Time to first occlusion, duration of first occlusion and thrombus size (ASA: 121974 µm² ± 77183 µm² vs. ASA + IPE: 161821 µm² ± 76925 µm², $p>0.05$) were unaltered (Fig. 5A and fig. S4A).

Second, we investigated arterial thrombosis in a carotid injury model in bone marrow chimeras reconstituted with bone marrow from endothelial and megakaryocytic *Cox-1*-deficient (*Ptgs1flox/flox;Tie2*-Cre) mice. In conditional *Cox-1*-deficient chimeric mice, there was no difference in time to first occlusion and duration of first occlusion of the carotid artery between IPE- and placebo-treated mice. Furthermore, maximal thrombus size did not differ between IPE- and placebo-treated mice (control: 230242 µm² ± 1278817 µm² vs. IPE: 178939 µm² ±

29361 µm², p>0.05). To rule out bone marrow transplantation and radiation associated effects on the platelet compartment and in vivo thrombus formation, chimeric mice reconstituted with bone marrow of wildtype mice were investigated. In these mice, IPE reduced time to first occlusion, duration of first occlusion and thrombus size in comparison to placebo-treated mice (control: 342748 µm² ± 68969 µm² vs. IPE: 191915 µm² ± 61610 µm², p=0.0283) in a comparable matter as in wildtype without bone marrow transplantation (Fig. 5B and fig. S4B). Knockout efficiency in platelets from chimeric mice was confirmed by western blotting (Fig. 5C). Histological analysis of formed thrombi did not reveal any difference between IPE- and placebo-treated mice (Fig. 5D and fig. S4C).

Switching from IPE to EPA/DHA-administration abolishes antiplatelet effects

To access lipidom alteration upon IPE supplementation we analyzed platelet lipid composition after ten days of IPE intake in patients. As expected, the amount of 20:5 containing lipids in the membrane increased indicating patients' intake compliance (Baseline (BL): 14.1 pmol/mg ± 13 pmol/mg vs. 10d: 63.7 pmol/mg ± 60.1 pmol/mg, p<0.0001) (Fig. 6A).

To evaluate the influence of IPE on platelet function, patient blood was analyzed before and ten days after intake of IPE (2g twice daily). Treatment with IPE suppressed platelet aggregation following stimulation with AA (Fig. 6B). Similarly, we observed decreased ATP-release, which is required for full-fledged platelet activation after IPE-intake (Fig. 6C). Furthermore, p-selectin expression as a marker for platelet degranulation was attenuated following AA- stimulation under IPE-intake (Fig. 6D).

In a second step, we investigated patients on IPE treatment who switched to EPA/DHA-medication (1g per day) (Fig. 6E). Reduced AA-induced platelet aggregation under IPE-treatment increased after ten days of EPA/DHA-intake (Fig. F6F). Subsequently, ATP-release increased after switching the medication (Fig. 6G) as well as AA-induced p-selectin expression (Fig. 6H*).*

EPA-derived oxylipins do not contribute to IPEs antiplatelet effects

To evaluate if changes in EPA-derived oxylipins may be responsible for EPA's antiplatelet effects we measured representative oxylipins derived from different oxygenases in human plasma after ten days of IPE-intake. We found a significant increase of 5-HEPE produced by 5-LOX ($p=0.0006$, fig. S5A), 12-HEPE produced by 12-LOX ($p=0.0034$, fig. S5B), 18-HEPE resulting from non-enzymatic oxidation of EPA ($p<0.0001$, fig. S5C) and 20-HEPE produced by CYP450 enzymes ($p<0.0001$,fig. S5D). Moreover, we found no significant difference in PGE3. PGE3 as an EPA-derived oxylipin produced by COX-1 pathway was below the detection limit in most of the samples (fig. S5E). In addition, we measured TXB2 after ten days of IPE-intake. We found decreased TXB2 amounts indicating COX-1-inhibition by EPA (fig. S5F). To investigate if these oxylipins might affect platelet function, we analyzed dose responses for LTA, p-selectin expression by flow cytometry, and ATP-release from healthy human platelets upon stimulation with the determined oxylipins. 5-HEPE did not affect aggregation and ATP-release, but increased P-selectin expression on a single platelet level at a concentration of 0.3 nM and 1.5 nM (fig. S6A to C). 12-HEPE, 18-HEPE and 20-HEPE did not affect aggregation, P-selectin expression, or ATP-release (fig. S6D to L). PGE3 did not alter aggregation (fig. S6M), reduced P-selectin expression following stimulation with 0.05 nM and 0.1 nM PGE3 (fig. S6N) and attenuated ATP-release at all tested concentrations (fig. S6O). To question whether endothelial cell COX-1 derived PGI2 or PGI3 may contribute to antiplatelet effects we measured 6-keto-PGF1a (a stable metabolite of PGI2) and delta17-6-keto-PGF1a (a stable metabolite of PGI3) after ten days of IPE-intake in plasma of patients. However, both metabolites could not be detected in were under the limit of detection, excluding a relevant role of EC derived PGIs.

Discussion

In this study, we identified an antithrombotic platelet derived mechanism under omega-3 polyunsaturated fatty acid supplementation with IPE providing translational evidence to current clinical trials.

A variety of clinical randomized trials assessed the efficiency of different omega-3 polyunsaturated fatty acid intake on cardiovascular effects and outcome. ASCEND(*2*), VITAL(*3*), and STRENGTH(*4*) failed to show a cardiovascular benefit of ω-3 PUFA supplementation. In contrast cardiovascular risk reduction was observed in the international REDUCE-IT (*5*) and the Japanese JELIS(*6*) trial that supplemented 2 g IPE twice daily or 1.8 g EPA once daily respectively.

Indeed, in REDUCE-IT, IPE supplementation yielded highest patient plasma level of EPA with median plasma concentration was 476 µM which could not be achieved by other ω-3 PUFA intake schemes (*4, 5*). Interestingly the STRENGTH-trial in which patients received a 4g EPA/DHA combination formulation yielded lower EPA plasma level (296 µM) while no cardiovascular benefits were found. Our dose-response measurements in vitro provide some insight on this, as addition of 250 µM EPA showed only a minor antiplatelet effect, suggesting high dosage regimes for EPA are needed to induce a clinically relevant thromboprotection. In addition our study provides experimental evidence that PUFA composition is crucial for antiplatelet effects.

Earlier in vitro studies reported stronger antiplatelet effects of DHA in comparison to EPA(*12*). However we found an augmented platelet reactivity upon switching from IPE to an EPA/DHA-formulation. Several aspects have to be considered. First, patients were supplemented with a clinically used EPA/DHA formulation, containing 460 mg EPA combined with 380 mg DHA once daily in contrast to guideline-recommended 2 g IPE twice daily dose(*13*). Second, in human DHA preferentially incorporates in cell membranes within the brain and the retina leading to an unequal distribution of EPA and DHA within the body potentially limiting the amount of DHA which can act at the platelet in vivo(*14*). Third, differences in the chemical

formulation affect pharmacokinetic properties(*15*). This is of particular interest given that combined ω-3 PUFA formulations contain EPA as carboxylic acid instead to as ethyl ester.

On a molecular level we found a competitive binding of EPA and AA to platelet COX-1 that eventually attenuates AA metabolization to prothrombotic TXA2 resulting in platelet inhibition. Of note, photoaffinity labeling and in silico docking analysis revealed similar binding affinities of AA and EPA to the active site of platelet COX-1, supporting our findings that EPA competitively interacts with AA at the active site of COX-1. Moreover, we demonstrated that EPA in vivo effects on arterial thrombosis depend on COX-1 underscoring the translational implications of our findings in patients on risk for atherothrombosis. To further support our hypothesis of an interaction between EPA and AA at the level of platelet COX-1, we showed that TXB2 amounts were decreased in vitro and ex vivo in human plasma after EPA-treatment. This is important as TXB2 is the stable metabolite of TXA2. TXA2 derives from AA through COX-1-metabolisation and is known to foster auto- and paracrine activation of platelets after activation(*16*). Therefore, a reduction in TXB2 goes in line with a reduced platelet reactivity. Moreover, reduction of TXB2 may be clinically relevant as high TXB2 concentrations are associated with cardiovascular events and therefore contribute to the risk reduction observed in REDUCE-IT and JELIS.(*17*)

Modulation of platelet membrane composition is known to modulate platelet function(*18*) and might occur under EPA supplementation. However, our data show that ratios of AA- and EPA-release from platelet membrane after activation did not change under IPE supplementation suggesting that additional incorporation of EPA into the platelet membrane is not a key driver of the observed antiplatelet effect. Moreover, we found that EPAs antiplatelet effect is independent from its triglyceride lowering effect. This is in line with a trial in which early administration of EPA after percutaneous coronary intervention in acute coronary syndrome leads to reduction of cardiovascular events without change in triglyceride concentration(*19*).

Platelet proteomics and phosphoproteomics revealed an influence of EPA on effector molecules in different pathways following platelet activation. This includes molecules which

are important for intracellular calcium release and the formation of cAMP as second messenger. Moreover, EPA also affects pathways that are not COX-1-associated like the vasodilator-stimulated phosphoprotein. These mediators are involved in auto- and paracrine augmentation of platelet activation. This underlines that EPA also affects the auto- and paracrine activation besides the inhibition of the initial platelet activation.

To address the impact of EPA-derived oxylipins on EPA's platelet inhibitory effects, we measured EPA-derived oxylipins in plasma in patients with cardiovascular disease and analyzed the effect of oxylipins on platelet function. Platelet reactivity was not affected by oxylipins derived from 5-LOX, 12-LOX, CYP450 and non-enzymatic oxidation. This goes in line with the current literature. Most evidence for the antiplatelet effects of these oxylipins is derived from in vitro studies with much higher concentrations in comparison to the measured concentration from human plasma in our study which are in nanomolar range. An IC_{50} of 25 µM was shown for 5-HETE(*20*), CYP450 derived oxylipins were shown to have an IC_{50} of about 5 µM(*21*) and for 12-HEPE a slight decrease of aggregation was shown with 20 µM(*22*). In contrast, we found that PGE3 affects degranulation in the concentration we measured in plasma at about 0.01 nM. This supports our hypothesis of EPA competing with AA at the active site of COX-1 resulting in inhibition of platelet function as PGE3 is an EPA/ COX-1-derived oxylipin. PGE3 contributes to EPAs antiplatelet effects only partly as merely dense granule degranulation is affected by a PGE3-concentration of 0.01 nM and alpha-granule release and platelet aggregation are not. Moreover, our data show that IPE intake does not lead to measurable concentrations of endothelial cell derived COX-1 metabolite PGI3 that may impact on thrombus formation. Of note the role of endothelial COX-1 derived metabolites was reported to be minor as genetic ablation of endothelial COX-1 in mice does not affect platelet function(*23*).

Besides the well-known effects of EPA regarding inflammation and lipid metabolism(*24*), we revealed a relevant antithrombotic effect. This leads to the conclusion that IPE as precursor of

EPA addresses residual risks in inflammation, lipid metabolism and thrombotic risk in addition to established optimal medical treatment in REDUCE-IT(*5, 25*).

Our study has several limitations. Sample size for human studies was small, precluding follow up for clinical events. Next, 6-keto-PGF1a and delta17-6-keto-PGF1a concentrations in humans after ten days of IPE-intake were under the limit of detection. PGE3 was also under the limit of detection in some samples. In addition, in vivo experiments were performed in male mice. However, there is no data available indicating a difference of effects of polyunsaturated fatty acids between different genders.

In summary our study provides mechanistic insights to the observed reduction of ischemic events in the REDUCE-IT and JELIS trials. In terms of safety, bleeding events in these two trials were just slightly higher in the intervention groups. Therefore, higher bleeding risk due to EPA-treatment may be negligible. We revealed an antithrombotic mechanism under ω-3 PUFA-supplementation with IPE resulting in platelet inhibition. This is of great importance as reasons for contradicting results between trials evaluating ω-3 PUFA are unclear. Our study adds evidence that concentration-dependent platelet inhibition by EPA may play a role in achieving cardiovascular risk reduction with EPA. Therefore, this study builds the base for further clinical trials investigating high dose EPA in patients with high risk for ischemic events.

Materials and Methods

Study design

The aim of this study was to evaluate potential antiplatelet effects of IPE mediated via COX-1-inhibition. We analyzed the effects of IPE on arterial thrombosis in wildtype and platelet *Cox-1*-deficient mice using a carotid injury model and a tail bleeding assay. The impact of IPE on platelet function in humans with cardiovascular disease was evaluated using flow chamber, aggregation, flow cytometry and an ATP-release assay in an observational study. The same methods were used for in vitro assessment of antiplatelet effects of EPA on human platelets from healthy donors. Twenty healthy donors were included and randomly assigned to the experiments. Moreover, lipidomics and phosphoproteomics were performed. At least four mice per group were used matched by age and genetic background with random assignment to the groups. There was no blinding for the investigators. All mouse studies were approved by the State Agency for Nature, Environment and Consumer Protection North Rhine-Westphalia, Germany (*Landesamt für Natur, Umwelt und Verbraucherschutz - LANUV NRW,* 81-02.04.2020.A319). Human studies were approved by the University of Düsseldorf Ethics Committee (No. 5823R).

Animals

Male C57BL/6J mice were purchased from Janvier Laboratory. All mice were 11-13 weeks old at the beginning of IPE-administration. Mice were fed a complete diet including 23% crude protein, 6% crude fat and 3.3% crude fiber from ssniff. IPE (TCI Chemicals) was administered by oral gavage every two days (2 g/kg body weight) for 14 days. If needed, ASA was administered via oral gavage 30 minutes prior to induction of arterial thrombosis (12.5 mg/kg body weight). If necessary, intravenous EPA was administered as emulsion in concentrations with 5 %, 10 % and 20 % EPA. Tween-20 was used as emulsifier and a volume of 150 µl was injected into the mice' tail vein.

In vivo arterial thrombus formation

Arterial thrombosis was induced by vessel injury using a Fe-(III)-chloride-soaked tissue. The tissue was placed at the outer surface of the arteria carotis communis. Visualization of platelets was ensured by injecting GPib-DYLight 488 tagged antibody (clone: X488, Emfret). For fluorescence microscopy, a Leica DM6FS was used. Evaluation of data was performed using Leica LASX software.

Tail bleeding assay

Mice were anesthetized with a mixture of ketamine (100 mg/kg BW) and xylazine (10 mg/kg BW). Mice were placed on a 37 °C heating plate in a prone position and a 5mm segment of the tail tip was amputated and dipped in a tube filled with 37 °C pre-warmed isotonic saline. Each animal was monitored for 30 minutes even if bleeding was interrupted to detect any re-bleedings. To analyze the bleeding volume, blood cells were separated by centrifugation at 1500 g for 5 min at room temperature. Erythrocytes were re-suspended and lysed in 2 ml of lysis buffer (pH 7.4) after the supernatant was discarded. After 10 minutes of incubation, tubes were centrifuged at 2000 g for 5 minutes. Haemoglobin concentration was measured spectrophotometrically at 550 nm. The volume of blood loss in each sample was calculated from a standard curve which was obtained by lysing defined volumes (0.3 – 300µl) of mouse blood. (*26, 27*)

Generation of bone marrow chimera

Cox-1-deficient chimeric mice were generated by radiation and following bone marrow transplantation (BMT) in wildtype mice. Recipient mice received two rounds of whole-body radiation (2 x 6.5 Gy) in an interval of 5 hours (Gulmay RS 225, 0.2 Cu, 175 kV). Purified bone marrow of *Cox-1*-knockout-mice (*Ptgs1flox/flox;Tie2*-Cre) was administered intravenously into the tail vein of recipient mice ($10x10^6$ cells/mouse) followed by three weeks of anti-infective prophylaxis with enrofloxacin (10 mg/kg BW). After this, the animals were given further three

weeks to recover. Chimerism was verified six weeks after transplantation by western blotting and flow cytometry-analysis.

Patients

We included 20 patients with first initiation of IPE (VASCEPA, Amarin) 2 grams twice daily due to elevated cardiovascular risk that we identified during routine practice at the division of cardiology of the University Hospital Dusseldorf. IPE was dosed according to the REDUCE-IT trial (2g twice daily). Blood sampling was conducted before the first intake and 10 days after beginning of supplementation. Exclusion criteria were antithrombotic medications, hematological diseases, malignant neoplasia, impaired kidney function, and age below 18 years. All patients gave informed written consent. In these patients, platelet function was assessed using light transmission aggregometry (LTA), flow cytometry, and adenosine-triphosphate (ATP)-release assay. We included 10 patients who had to change from IPE to an EPA/DHA (460 mg EPA and 380 mg DHA) combination formulation since VASCEPA (Amarin) is no longer paid by health insurances in Germany. Again, we assessed platelet function using LTA, ATP-release assay, and flow cytometry. Platelets were analyzed at the last day of IPE treatment and ten days after switching to EPA/DHA. Adherence to medication was monitored by personal interview. Furthermore, we included 370 patients in a monocentric all-comers study at the division of cardiology of the University Hospital Duesseldorf. Inclusion criteria were ASA medication and informed consent. Exclusion criteria were hematological diseases and age below 18 years. We evaluated platelet function using LTA in these patients and correlated with plasma triglycerides. Patients' characteristics are given in table S1.

Statistical analysis

Statistical analyses were conducted using IBM SPSS-Software and GraphPad-Prism statistical software (GraphPad Software Inc). Normality of distribution was tested with Kolmogorov-Smirnov test, D'Agostino-Pearson test, qq-plots and histograms. Normally distributed continuous variables were analyzed using the t-test; non-normally distributed variables using the Mann-Whitney U test. Comparison of three or more groups was performed

using ANOVA-analysis, Friedman-test or mixed-effect-analysis in dependence of normal distribution. For post-hoc analysis, Dunnett's and Dunn's test were used. P values below 0.05 were defined significant.

Acknowledgements:

We thank Kirsten Bartkowski for her experimental support. FAS and AS thank Dr. Dominik Kopczynski for the development of the bioinformatics platform Innt and Ms. Svenja Ideal for technical support.

Funding

This work was supported by the Forschungskommission of the Medical Faculty of the Heinrich Heine University (No 46-2016 to L.D. and 29-2019 to L.D.; No. 16-2014 to A.P. and 18-2019 to A.P., No. 2020-51 to C.H., No. 2021-01 to P.M.), funded by the Deutsche Forschungsgemeinschaft (DFG, German Research Foundation) – grant no 493659010 to P.M, grant no. 530690968 to M.B., grant no. 236177352-SFB1116, TP B11 to A.P. and TP B11 to B.L, TP B09 to N.G, TP B6 to M.K. and B12 to M.K., grant no. 493400536 to A.P., 413659045 to A.P, and 510844896 to A.P, grant no. PE2704/3-1 to T.P., PE2704/4-1 to T.P. and PE2704/5-1 to T.P., by the Susanne-Bunnenberg-Stiftung at the Duesseldorf Heart Center, the DZHK (German Center for Cardiovascular Research) to A.P. and T.P. (external cooperation grant) and DZHK-BHF-DHF funding (MEGACARDIOCYTE) to T.P., the Bundesministerium für Bildung und Forschung (BMBF) (to A.S., F.S., D.K. and S.V.) and by the Ministerium für Kultur und Wissenschaft des Landes Nordrhein-Westfalen (to A.S., F.S., D.K. and S.V.).

Author contributions

P.M. supervised the study, wrote the manuscript, planned experiments and analyzed data. M.B. supervised the study and performed mouse studies. L.W. performed in vitro experiments and performed literature research. M.B. performed animal studies. C.H. supervised the study, wrote the manuscript, reviewed and edited the manuscript. C.C. performed in vitro

experiments. F.S. performed in vitro experiments. D.K. performed in vitro experiments. L.D. supervised the study, performed literature research and analyzed the data. S.A., D.Z., A.U., K.T., H.R., G.A., R.M. and S.Z. performed in vitro experiments. S.P. supervised mouse experiments. N.G. supervised the study and reviewed the manuscript. C.D., J.P., Z.Z., M.T., Q.A. and P.K. performed in vitro experiments. N.K. provided murine bone marrow for transplantation. D.S. performed mouse experiments. W.B. supervised mouse experiments. T.H., K.S., B.L., T.Z., S.V., R.A., A.S., J.M., U.L., S.M. and M.K. supervised the study, revised the manuscript and provided laboratory spaces and materials. S.M., J.M. and D. B. supervised the study and revised the manuscript. T.P. supervised the study, reviewed the manuscript, planned the study and provided laboratory space and materials. A.P. supervised and designed the study, reviewed the manuscript, designed the research and analyzed the data.

Competing interests:

Dr. Bhatt discloses the following relationships - Advisory Board: AngioWave, Bayer, Boehringer Ingelheim, Cardax, CellProthera, Cereno Scientific, Elsevier Practice Update Cardiology, High Enroll, Janssen, Level Ex, McKinsey, Medscape Cardiology, Merck, MyoKardia, NirvaMed, Novo Nordisk, PhaseBio, PLx Pharma, Regado Biosciences, Stasys; Board of Directors: AngioWave (stock options), Boston VA Research Institute, Bristol Myers Squibb (stock), DRS.LINQ (stock options), High Enroll (stock), Society of Cardiovascular Patient Care, TobeSoft; Chair: Inaugural Chair, American Heart Association Quality Oversight Committee; Consultant: Broadview Ventures; Data Monitoring Committees: Acesion Pharma, Assistance Publique-Hôpitaux de Paris, Baim Institute for Clinical Research (formerly Harvard Clinical Research Institute, for the PORTICO trial, funded by St. Jude Medical, now Abbott), Boston Scientific (Chair, PEITHO trial), Cleveland Clinic (including for the ExCEED trial, funded by Edwards), Contego Medical (Chair, PERFORMANCE 2), Duke Clinical Research Institute, Mayo Clinic, Mount Sinai School of Medicine (for the ENVISAGE trial, funded by Daiichi Sankyo; for the ABILITY-DM trial, funded by Concept Medical), Novartis, Population Health Research Institute; Rutgers University (for the NIH-funded MINT Trial); Honoraria: American

College of Cardiology (Senior Associate Editor, Clinical Trials and News, ACC.org; Chair, ACC Accreditation Oversight Committee), Arnold and Porter law firm (work related to Sanofi/Bristol-Myers Squibb clopidogrel litigation), Baim Institute for Clinical Research (formerly Harvard Clinical Research Institute; RE-DUAL PCI clinical trial steering committee funded by Boehringer Ingelheim; AEGIS-II executive committee funded by CSL Behring), Belvoir Publications (Editor in Chief, Harvard Heart Letter), Canadian Medical and Surgical Knowledge Translation Research Group (clinical trial steering committees), Cowen and Company, Duke Clinical Research Institute (clinical trial steering committees, including for the PRONOUNCE trial, funded by Ferring Pharmaceuticals), HMP Global (Editor in Chief, Journal of Invasive Cardiology), Journal of the American College of Cardiology (Guest Editor; Associate Editor), K2P (Co-Chair, interdisciplinary curriculum), Level Ex, Medtelligence/ReachMD (CME steering committees), MJH Life Sciences, Oakstone CME (Course Director, Comprehensive Review of Interventional Cardiology), Piper Sandler, Population Health Research Institute (for the COMPASS operations committee, publications committee, steering committee, and USA national co-leader, funded by Bayer), Slack Publications (Chief Medical Editor, Cardiology Today's Intervention), Society of Cardiovascular Patient Care (Secretary/Treasurer), WebMD (CME steering committees), Wiley (steering committee); Other: Clinical Cardiology (Deputy Editor), NCDR-ACTION Registry Steering Committee (Chair), VA CART Research and Publications Committee (Chair); Patent: Sotagliflozin (named on a patent for sotagliflozin assigned to Brigham and Women's Hospital who assigned to Lexicon; neither I nor Brigham and Women's Hospital receive any income from this patent); Research Funding: Abbott, Acesion Pharma, Afimmune, Aker Biomarine, Amarin, Amgen, AstraZeneca, Bayer, Beren, Boehringer Ingelheim, Boston Scientific, Bristol-Myers Squibb, Cardax, CellProthera, Cereno Scientific, Chiesi, CinCor, CSL Behring, Eisai, Ethicon, Faraday Pharmaceuticals, Ferring Pharmaceuticals, Forest Laboratories, Fractyl, Garmin, HLS Therapeutics, Idorsia, Ironwood, Ischemix, Janssen, Javelin, Lexicon, Lilly, Medtronic, Merck, Moderna, MyoKardia, NirvaMed, Novartis, Novo Nordisk, Owkin, Pfizer, PhaseBio, PLx Pharma, Recardio, Regeneron, Reid Hoffman Foundation, Roche, Sanofi, Stasys, Synaptic, The Medicines Company, Youngene,

89Bio; Royalties: Elsevier (Editor, Braunwald's Heart Disease); Site Co-Investigator: Abbott, Biotronik, Boston Scientific, CSI, Endotronix, St. Jude Medical (now Abbott), Philips, SpectraWAVE, Svelte, Vascular Solutions; Trustee: American College of Cardiology; Unfunded Research: FlowCo, Takeda. The remaining authors declare no conflict of interests.

Data and materials availability

All data associated with this study are present in the paper or supplementary materials.

List of Supplementary Materials

Materials and methods

Figures S1 – S7

Table S1

References (*28-45*)

MDAR Reproducibility checklist

References:

1. H. O. Bang, J. Dyerberg, A. B. Nielsen, Plasma lipid and lipoprotein pattern in Greenlandic West-coast Eskimos. *Lancet* **1**, 1143-1145 (1971).
2. A. S. C. Group, L. Bowman, M. Mafham, K. Wallendszus, W. Stevens, G. Buck, J. Barton, K. Murphy, T. Aung, R. Haynes, J. Cox, A. Murawska, A. Young, M. Lay, F. Chen, E. Sammons, E. Waters, A. Adler, J. Bodansky, A. Farmer, R. McPherson, A. Neil, D. Simpson, R. Peto, C. Baigent, R. Collins, S. Parish, J. Armitage, Effects of n-3 Fatty Acid Supplements in Diabetes Mellitus. *N Engl J Med* **379**, 1540-1550 (2018).
3. J. E. Manson, N. R. Cook, I. M. Lee, W. Christen, S. S. Bassuk, S. Mora, H. Gibson, D. Gordon, T. Copeland, D. D'Agostino, G. Friedenberg, C. Ridge, V. Bubes, E. L. Giovannucci, W. C. Willett, J. E. Buring, V. R. Group, Vitamin D Supplements and Prevention of Cancer and Cardiovascular Disease. *N Engl J Med* **380**, 33-44 (2019).
4. S. J. Nicholls, A. M. Lincoff, M. Garcia, D. Bash, C. M. Ballantyne, P. J. Barter, M. H. Davidson, J. J. P. Kastelein, W. Koenig, D. K. McGuire, D. Mozaffarian, P. M. Ridker, K. K. Ray, B. G. Katona, A. Himmelmann, L. E. Loss, M. Rensfeldt, T. Lundstrom, R. Agrawal, V. Menon, K. Wolski, S. E. Nissen, Effect of High-Dose Omega-3 Fatty Acids vs Corn Oil on Major Adverse Cardiovascular Events in Patients at High Cardiovascular Risk: The STRENGTH Randomized Clinical Trial. *JAMA* **324**, 2268-2280 (2020).
5. D. L. Bhatt, P. G. Steg, M. Miller, E. A. Brinton, T. A. Jacobson, S. B. Ketchum, R. T. Doyle, Jr., R. A. Juliano, L. Jiao, C. Granowitz, J. C. Tardif, C. M. Ballantyne, R.-I. Investigators, Cardiovascular Risk Reduction with Icosapent Ethyl for Hypertriglyceridemia. *N Engl J Med* **380**, 11-22 (2019).
6. M. Yokoyama, H. Origasa, M. Matsuzaki, Y. Matsuzawa, Y. Saito, Y. Ishikawa, S. Oikawa, J. Sasaki, H. Hishida, H. Itakura, T. Kita, A. Kitabatake, N. Nakaya, T. Sakata, K. Shimada, K. Shirato, E. P. A. l. i. s. I. Japan, Effects of eicosapentaenoic acid on major coronary events in hypercholesterolaemic patients (JELIS): a randomised open-label, blinded endpoint analysis. *Lancet* **369**, 1090-1098 (2007).
7. X. Wang, S. Verma, R. P. Mason, D. L. Bhatt, The Road to Approval: a Perspective on the Role of Icosapent Ethyl in Cardiovascular Risk Reduction. *Curr Diab Rep* **20**, 65 (2020).
8. L. J. Marnett, S. W. Rowlinson, D. C. Goodwin, A. S. Kalgutkar, C. A. Lanzo, Arachidonic acid oxygenation by COX-1 and COX-2. Mechanisms of catalysis and inhibition. *J Biol Chem* **274**, 22903-22906 (1999).
9. H. Arita, T. Nakano, K. Hanasaki, Thromboxane A2: its generation and role in platelet activation. *Prog Lipid Res* **28**, 273-301 (1989).

10. G. Kobzar, V. Mardla, I. Jarving, N. Samel, Comparison of anti-aggregatory effects of PGI2, PGI3 and iloprost on human and rabbit platelets. *Cell Physiol Biochem* **11**, 279-284 (2001).
11. J. Yeung, M. Hawley, M. Holinstat, The expansive role of oxylipins on platelet biology. *J Mol Med (Berl)* **95**, 575-588 (2017).
12. M. Lagarde, C. Calzada, M. Guichardant, E. Vericel, In vitro and in vivo bimodal effects of docosahexaenoic acid supplements on redox status and platelet function. *Prostaglandins Leukot Essent Fatty Acids* **138**, 60-63 (2018).
13. F. L. J. Visseren, F. Mach, Y. M. Smulders, D. Carballo, K. C. Koskinas, M. Back, A. Benetos, A. Biffi, J. M. Boavida, D. Capodanno, B. Cosyns, C. Crawford, C. H. Davos, I. Desormais, E. Di Angelantonio, O. H. Franco, S. Halvorsen, F. D. R. Hobbs, M. Hollander, E. A. Jankowska, M. Michal, S. Sacco, N. Sattar, L. Tokgozoglu, S. Tonstad, K. P. Tsioufis, I. van Dis, I. C. van Gelder, C. Wanner, B. Williams, E. S. C. N. C. Societies, E. S. C. S. D. Group, 2021 ESC Guidelines on cardiovascular disease prevention in clinical practice. *Eur Heart J* **42**, 3227-3337 (2021).
14. R. P. Mason, P. Libby, D. L. Bhatt, Emerging Mechanisms of Cardiovascular Protection for the Omega-3 Fatty Acid Eicosapentaenoic Acid. *Arterioscler Thromb Vasc Biol* **40**, 1135-1147 (2020).
15. L. Chevalier, M. Plourde, Comparison of pharmacokinetics of omega-3 fatty acid supplements in monoacylglycerol or ethyl ester in humans: a randomized controlled trial. *Eur J Clin Nutr* **75**, 680-688 (2021).
16. V. Capra, M. Back, D. J. Angiolillo, M. Cattaneo, K. S. Sakariassen, Impact of vascular thromboxane prostanoid receptor activation on hemostasis, thrombosis, oxidative stress, and inflammation. *J Thromb Haemost* **12**, 126-137 (2014).
17. D. Pastori, P. Pignatelli, A. Farcomeni, R. Cangemi, W. R. Hiatt, S. Bartimoccia, C. Nocella, T. Vicario, T. Bucci, R. Carnevale, G. Y. Lip, F. Violi, Urinary 11-dehydro-thromboxane B2 is associated with cardiovascular events and mortality in patients with atrial fibrillation. *Am Heart J* **170**, 490-497 e491 (2015).
18. M. V. Selvadurai, R. J. Brazilek, M. J. Moon, J. Y. Rinckel, A. Eckly, C. Gachet, P. J. Meikle, H. H. Nandurkar, W. S. Nesbitt, J. R. Hamilton, The PI 3-kinase PI3KC2alpha regulates mouse platelet membrane structure and function independently of membrane lipid composition. *FEBS Lett* **593**, 88-96 (2019).
19. K. Nosaka, T. Miyoshi, M. Iwamoto, M. Kajiya, K. Okawa, S. Tsukuda, F. Yokohama, M. Sogo, T. Nishibe, N. Matsuo, S. Hirohata, H. Ito, M. Doi, Early initiation of eicosapentaenoic acid and statin treatment is associated with better clinical outcomes than statin alone in patients with acute coronary syndromes: 1-year outcomes of a randomized controlled study. *Int J Cardiol* **228**, 173-179 (2017).
20. D. E. Mais, D. L. Saussy, Jr., D. E. Magee, N. L. Bowling, Interaction of 5-HETE, 12-HETE, 15-HETE and 5,12-diHETE at the human platelet thromboxane A2/prostaglandin H2 receptor. *Eicosanoids* **3**, 121-124 (1990).
21. E. Hill, F. Fitzpatrick, R. C. Murphy, Biological activity and metabolism of 20-hydroxyeicosatetraenoic acid in the human platelet. *Br J Pharmacol* **106**, 267-274 (1992).
22. K. N. Ikei, J. Yeung, P. L. Apopa, J. Ceja, J. Vesci, T. R. Holman, M. Holinstat, Investigations of human platelet-type 12-lipoxygenase: role of lipoxygenase products in platelet activation. *J Lipid Res* **53**, 2546-2559 (2012).
23. J. A. Mitchell, F. Shala, M. E. L. Pires, R. Y. Loy, A. Ravendren, J. Benson, P. Urquhart, A. Nicolaou, H. R. Herschman, N. S. Kirkby, Endothelial cyclooxygenase-1 paradoxically drives local vasoconstriction and atherogenesis despite underpinning prostacyclin generation. *Sci Adv* **7**, (2021).
24. T. D. O'Connell, R. P. Mason, M. J. Budoff, A. M. Navar, G. C. Shearer, Mechanistic insights into cardiovascular protection for omega-3 fatty acids and their bioactive lipid metabolites. *Eur Heart J Suppl* **22**, J3-J20 (2020).

25. D. L. Bhatt, P. G. Steg, M. Miller, E. A. Brinton, T. A. Jacobson, S. B. Ketchum, R. T. Doyle, Jr., R. A. Juliano, L. Jiao, C. Granowitz, J. C. Tardif, C. M. Ballantyne, R.-I. Investigators, Cardiovascular Risk Reduction with Icosapent Ethyl for Hypertriglyceridemia. *N Engl J Med*, (2018).
26. Y. Liu, N. L. Jennings, A. M. Dart, X. J. Du, Standardizing a simpler, more sensitive and accurate tail bleeding assay in mice. *World J Exp Med* **2**, 30-36 (2012).
27. S. Ferriere, I. Peyron, O. D. Christophe, C. Kawecki, C. Casari, V. Muczynski, A. Nathwani, A. Kauskot, P. J. Lenting, C. V. Denis, A hemophilia A mouse model for the in vivo assessment of emicizumab function. *Blood* **136**, 740-748 (2020).
28. R. Brandl, T. Richter, K. Haug, M. G. Wilhelm, P. C. Maurer, W. Nathrath, Topographic analysis of proliferative activity in carotid endarterectomy specimens by immunocytochemical detection of the cell cycle-related antigen Ki-67. *Circulation* **96**, 3360-3368 (1997).
29. J. J. Thiessen, Aspirin: plasma concentration and effects. *Thromb Res Suppl* **4**, 105-111 (1983).
30. J. Nagelschmitz, M. Blunck, J. Kraetzschmar, M. Ludwig, G. Wensing, T. Hohlfeld, Pharmacokinetics and pharmacodynamics of acetylsalicylic acid after intravenous and oral administration to healthy volunteers. *Clin Pharmacol* **6**, 51-59 (2014).
31. S. N. Jayasinghe, Reimagining Flow Cytometric Cell Sorting. *Adv Biosyst* **4**, e2000019 (2020).
32. A. Assinger, I. Volf, D. Schmid, A novel, rapid method to quantify intraplatelet calcium dynamics by ratiometric flow cytometry. *PLoS One* **10**, e0122527 (2015).
33. J. A. Erhardt, K. Pillarisetti, J. R. Toomey, Potentiation of platelet activation through the stimulation of P2X1 receptors. *J Thromb Haemost* **1**, 2626-2635 (2003).
34. J. H. Cho, G. D. Wool, M. Y. Tjota, J. Gutierrez, K. Mikrut, J. L. Miller, Functional Assessment of Platelet Dense Granule ATP Release. *Am J Clin Pathol* **155**, 863-872 (2021).
35. L. Wang, Y. Li, R. Guo, S. Li, A. Chang, Z. Zhu, P. Tu, Optimized bioluminescence analysis of adenosine triphosphate (ATP) released by platelets and its application in the high throughput screening of platelet inhibitors. *PLoS One* **14**, e0223096 (2019).
36. C. A. Schneider, W. S. Rasband, K. W. Eliceiri, NIH Image to ImageJ: 25 years of image analysis. *Nat Methods* **9**, 671-675 (2012).
37. J. M. Burkhart, C. Schumbrutzki, S. Wortelkamp, A. Sickmann, R. P. Zahedi, Systematic and quantitative comparison of digest efficiency and specificity reveals the impact of trypsin quality on MS-based proteomics. *J Proteomics* **75**, 1454-1462 (2012).
38. H. Post, R. Penning, M. A. Fitzpatrick, L. B. Garrigues, W. Wu, H. D. MacGillavry, C. C. Hoogenraad, A. J. Heck, A. F. Altelaar, Robust, Sensitive, and Automated Phosphopeptide Enrichment Optimized for Low Sample Amounts Applied to Primary Hippocampal Neurons. *J Proteome Res* **16**, 728-737 (2017).
39. J. V. Olsen, L. M. de Godoy, G. Li, B. Macek, P. Mortensen, R. Pesch, A. Makarov, O. Lange, S. Horning, M. Mann, Parts per million mass accuracy on an Orbitrap mass spectrometer via lock mass injection into a C-trap. *Mol Cell Proteomics* **4**, 2010-2021 (2005).
40. D. N. Perkins, D. J. Pappin, D. M. Creasy, J. S. Cottrell, Probability-based protein identification by searching sequence databases using mass spectrometry data. *Electrophoresis* **20**, 3551-3567 (1999).
41. C. R. Pelz, M. Kulesz-Martin, G. Bagby, R. C. Sears, Global rank-invariant set normalization (GRSN) to reduce systematic distortions in microarray data. *BMC Bioinformatics* **9**, 520 (2008).
42. S. Forli, R. Huey, M. E. Pique, M. F. Sanner, D. S. Goodsell, A. J. Olson, Computational protein-ligand docking and virtual drug screening with the AutoDock suite. *Nat Protoc* **11**, 905-919 (2016).

43. O. Trott, A. J. Olson, AutoDock Vina: improving the speed and accuracy of docking with a new scoring function, efficient optimization, and multithreading. *J Comput Chem* **31**, 455-461 (2010).
44. G. Rimon, R. S. Sidhu, D. A. Lauver, J. Y. Lee, N. P. Sharma, C. Yuan, R. A. Frieler, R. C. Trievel, B. R. Lucchesi, W. L. Smith, Coxibs interfere with the action of aspirin by binding tightly to one monomer of cyclooxygenase-1. *Proc Natl Acad Sci U S A* **107**, 28-33 (2010).
45. M. G. Malkowski, S. L. Ginell, W. L. Smith, R. M. Garavito, The productive conformation of arachidonic acid bound to prostaglandin synthase. *Science* **289**, 1933-1937 (2000).

Figures:

Figure 1: Icosapent ethyl (IPE) reduced arterial thrombus formation *in vivo.*

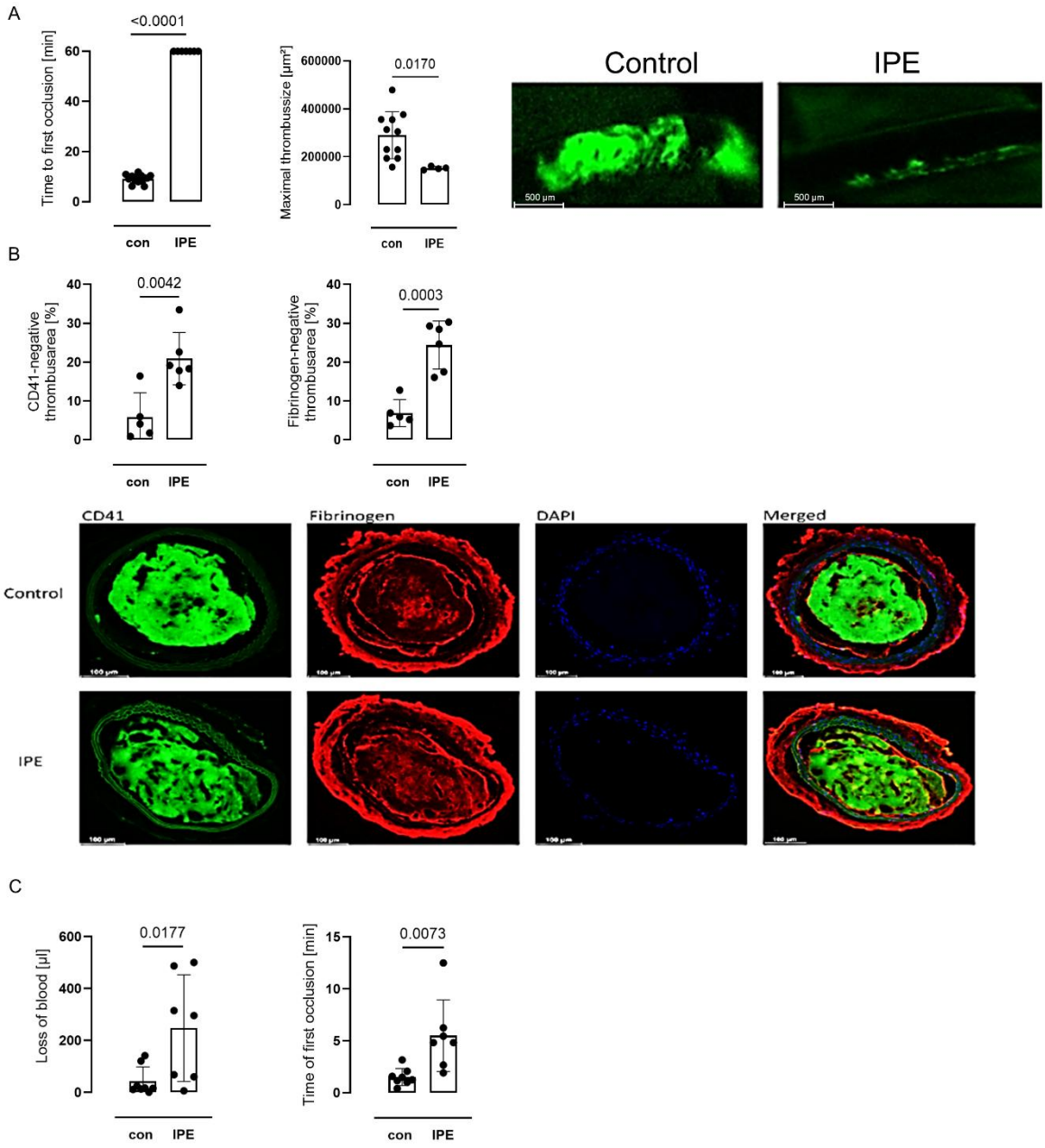

A) The bar plots show time to first occlusion (left, unpaired t-test, p>0.0001, $n_{control}$=15, n_{IPE}=7, data are means ± SD) and maximal thrombus size (middle, unpaired t-test, p=0.0170, $n_{control}$=15, n_{IPE}=7, data are means ± SD) in in vivo arterial thrombus formation model using the carotid artery injury model in wildtype mice. Representative pictures of arterial thrombi (right) show intravascular thrombi in green (control on the left and IPE-treated mice on the right, scale bars indicate 500 µm) B) The plots show CD41-negative thrombus area (left, unpaired t-test, p=0.0042, $n_{control}$=5, n_{IPE}=6, data are means ± SD) and fibrinogen-negative thrombus area (right, unpaired t-test, p=0.0003, $n_{control}$=5, n_{IPE}=6, data are means ± SD) for histological analysis of carotid thrombi after carotid artery injury model in wildtype mice. Representative histological images (below) show CD41 in green, fibrinogen in red, and DAPI stained nuclei in blue. Control is shown in the upper line and IPE-treatment is shown below. Scale bars are given for 100µM. C) The bar plots show loss of blood (left, unpaired t-test, n=7, p=0.0177, data

are means ± SD) and bleeding time (right, unpaired t-test, n=7, p=0.0073, data are means ± SD) in a tail bleeding assay in mice treated with IPE or placebo.

Figure 2: Eicosapentaenoic acid (EPA) inhibited platelet adhesion, aggregation, degranulation and intracellular calcium-signaling in a concentration-dependent manner.

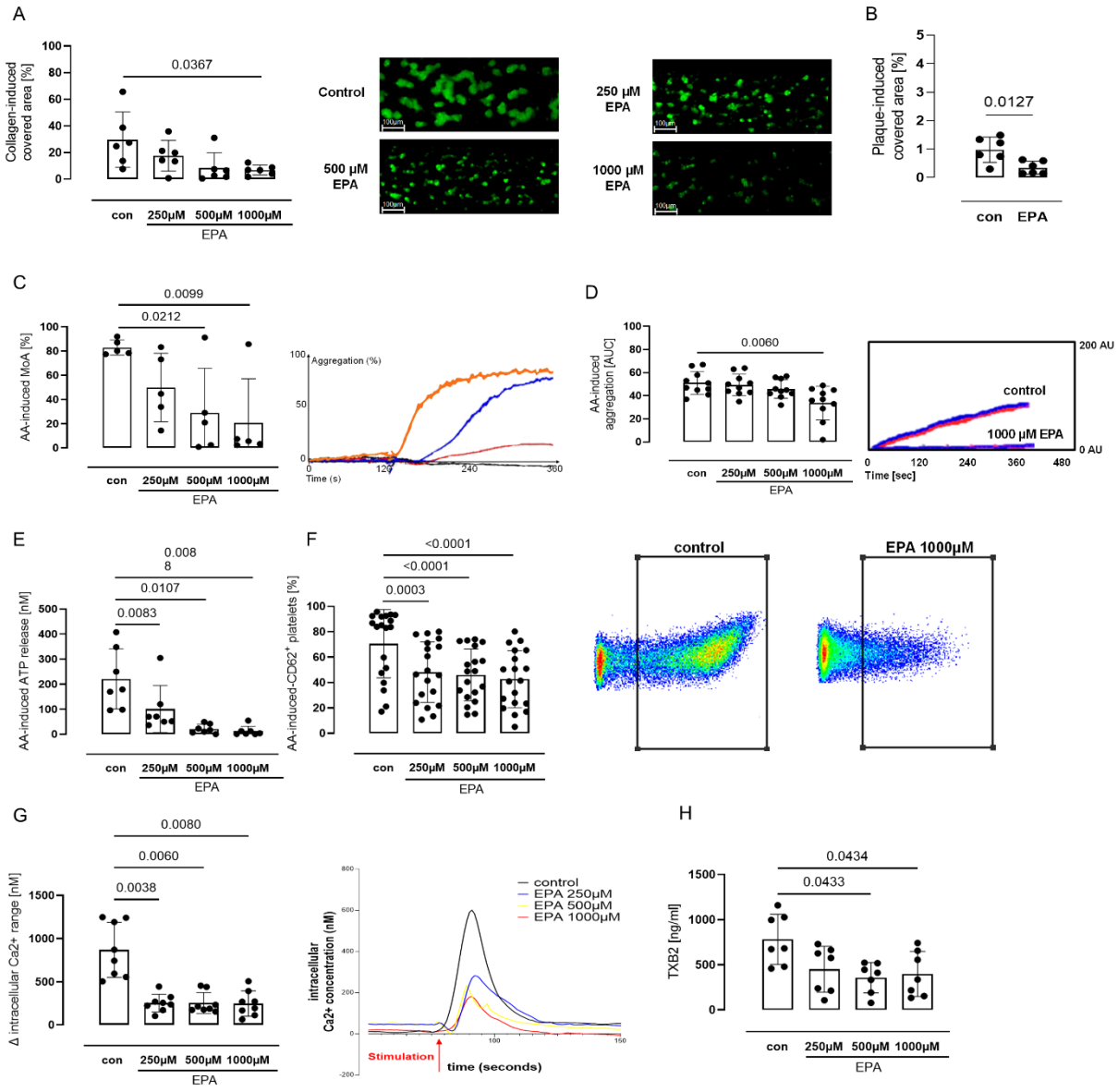

A) The bar plots show platelet adhesion of human platelets in vitro on a collagen-coated flow chamber (ANOVA-analysis, p=0.0345; Dunnett's test for multiple comparison: control vs. 1000 µM EPA: p=0.0367, n=6, data are means ± SD). Representative images of the flow chamber are shown on the right. Green fluorescence indicates platelets. Control is shown upper left, 250 µM EPA in the upper right, 500 µM EPA in the lower left and 1000 µM EPA in the lower right box. B) The bar plots show platelet adhesion on human plaque material (paired t-test, p=0.0127, n=6, data are means ± SD) C) The bar plots show platelet aggregation in light transmission aggregometry induced by arachidonic acid (AA) (Friedman-test, p=0.0055, Multiple comparison with Dunn's correction, con vs. 500 µM: p=0.0212, con vs. 1000 µM: p=0.0099, n=5, data are means ± SD). Representative analysis is shown on the right (orange = control, blue = 250 µM EPA, red = 500 µM EPA and black = 1000 µM EPA) D) The bar plots

show AA-induced platelet aggregation in impedance aggregometry (ANOVA-analysis, p=0.0017, Dunnett's multiple comparison test, control vs. 1000 µM EPA: p=0.0060, n=10, data are means ± SD). Representative aggregation curves for control and 1000 µM EPA are shown on the right. E) The bar plots show AA-induced adenosine triphosphate (ATP) release from human platelets (ANOVA-analysis, p=0.0031, Dunnett's multiple comparison test, control vs. 250 µM EPA: p=0.0083, control vs. 500 µM EPA: p=0.0107, control vs. 1000 µM EPA: p=0.0088, n=7, data are means ± SD). F) The bar plots show AA-induced p-selectin expression on human platelets (ANOVA-analysis, p<0.0001; Dunnett's multiple comparison test, control vs. 250 µM EPA: p=0.0003, control vs. 500 µM EPA: p<0.0001, control vs. 1000 µM EPA: p<0.0001, n=19, data are means ± SD). Representative flow cytometry-plots are shown on the right (control on the left, and 1000 µM EPA on the right). G) The bar plots show delta of transcellular calcium-concentration in human platelet after stimulation (ANOVA-analysis, p=0.0004; Dunnett's multiple comparison test, control vs. 250 µM EPA: p=0.0038, control vs. 500 µM EPA: p=0.0060, control vs. 1000 µM EPA: p=0.0080, n=8, data are means ± SD). Representative plot of intracellular calcium changes is shown on the right (black = control, blue = 250 µM EPA, yellow = 500 µM EPA, red = 1000 µM EPA). H) The bar plots show AA-induced TXB2-production from human platelets in vitro (ANOVA-analysis, p=0.0118, Dunnett's multiple comparison test, control vs. 500 µM EPA: p=0.0433; control vs. 1000µM EPA: p=0.0434, n=7, data are means ± SD).

Figure 3: Eicosapentaenoic acid (EPA) abolished the effect of arachidonic acid (AA) on platelet proteomics and phosphoproteomics in various intracellular signaling pathways.

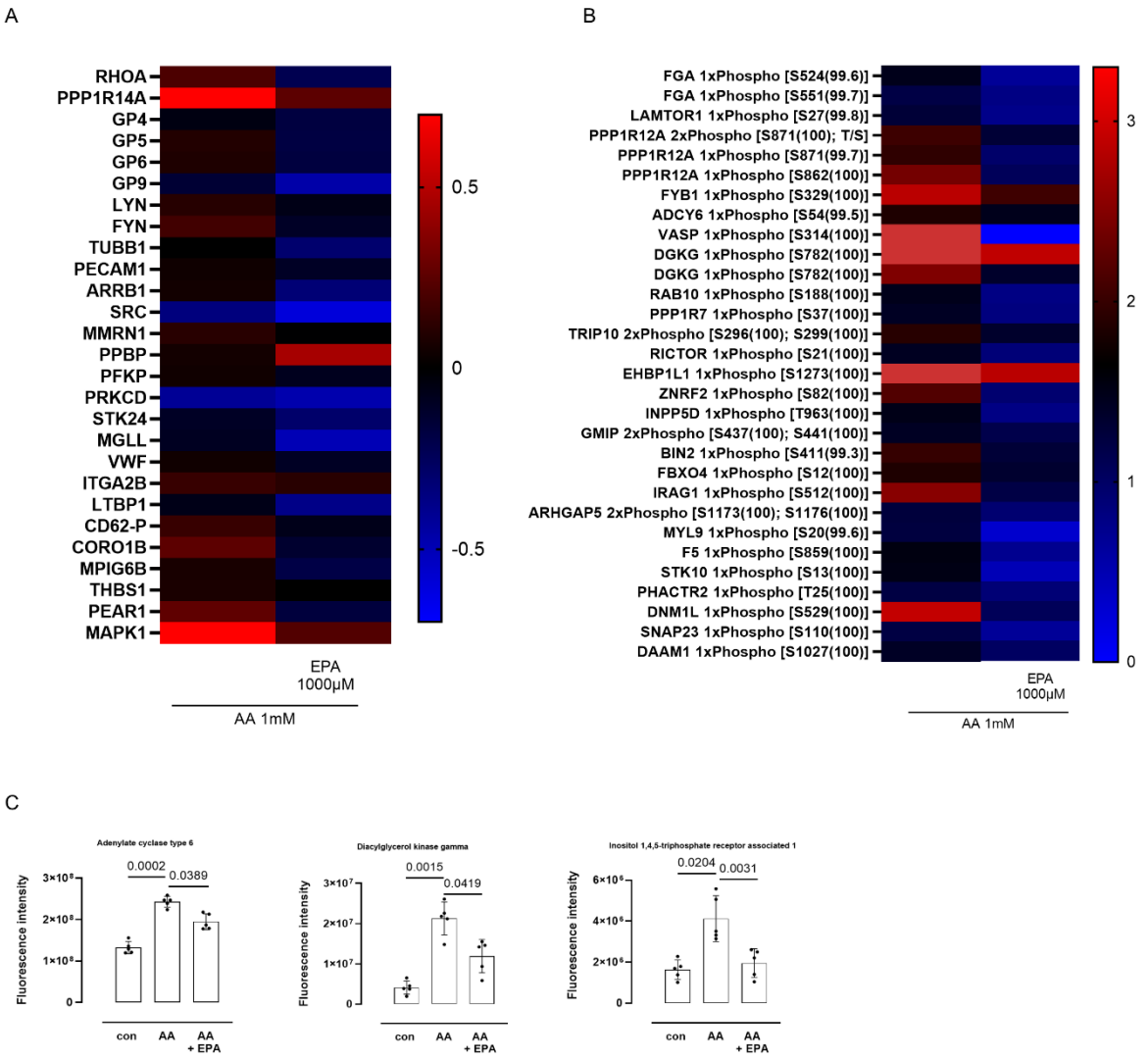

A) Heat map representing the proteome changes in comparison of AA-stimulation and AA-stimulation with EPA-treatment. Scale bar indicates fold change in comparison to untreated control. B) Heat map representing phosphoproteomic changes in comparison of AA-stimulation and AA-stimulation with EPA-treatment. Proteins are given with phosphorylation sites on the left axis. Scale bar on the right side indicates fold change in comparison to untreated control. C) The bar plots show regulated proteins in different intracellular signaling pathways in human platelets with control treatment, AA-stimulation and AA-stimulation with EPA-treatment. Adenylate cyclase type 6 (left, p=0.0007, con vs: AA: p= 0.0002, AA vs. AA + EPA: p=0.0389, n=5, data are means ± SD), diacylglycerol kinase gamma (middle, p=0.0007, con vs. AA: p=0.0015, AA vs AA + EPA: p=0.0419 n=5, data are means ± SD), inositol 1, 4, 5-triphsophate receptor associated 1 (right, p=0.0052, con vs. AA: p=0.0204, AA vs. AA + EPA: p=0.0031 n=5, data are means ± SD) (all ANOVA-analysis and Dunnett's test for multiple comparison).

Figure 4: Eicosapentaenoic acid (EPA) and arachidonic acid (AA) interacted competitively at the active site of platelet cyclooxygenase (COX)-1.

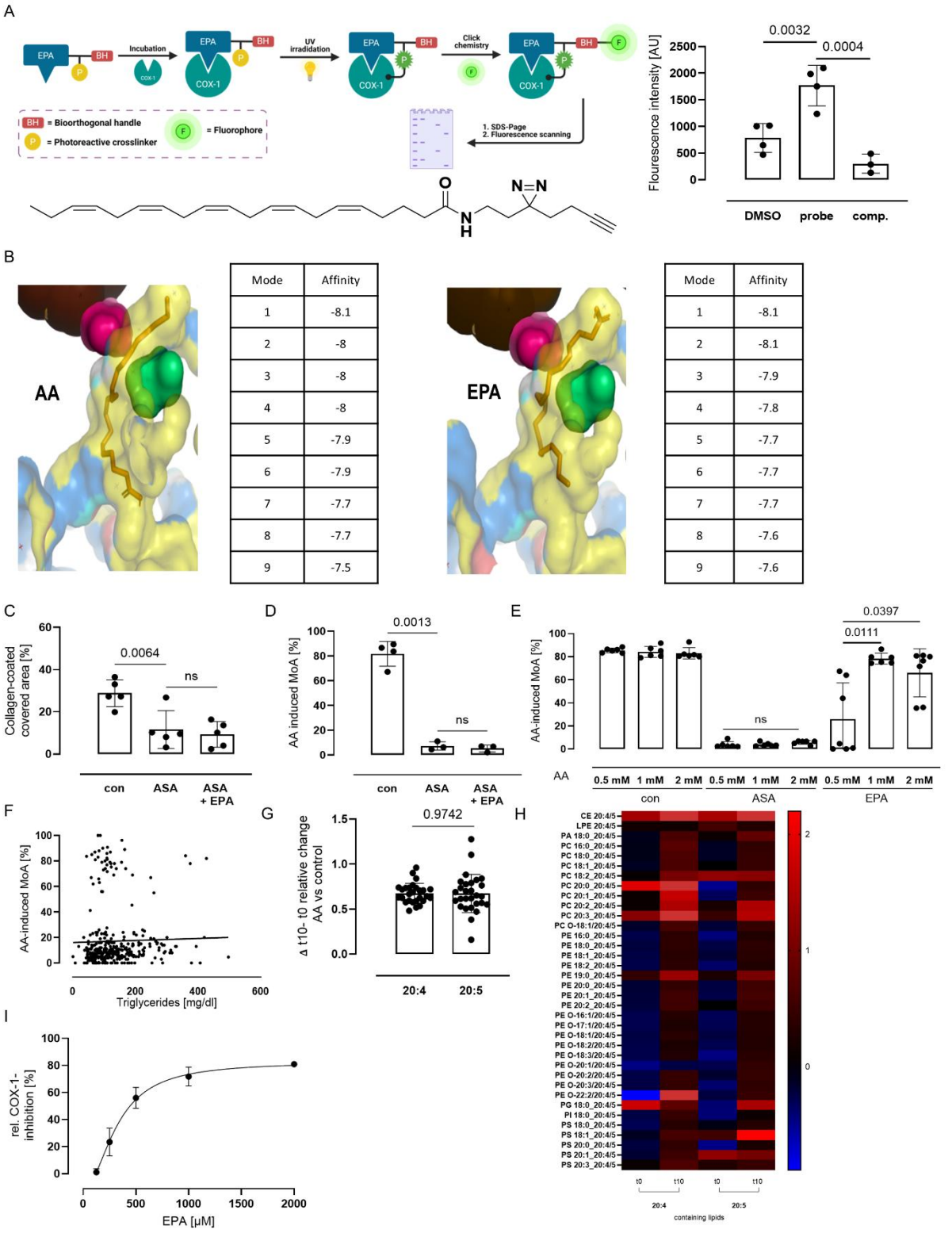

A) The schematic (left) shows the experimental design of photo affinity labeling. The bar plot (right) shows fluorescence intensity of control compared with the probe (ANOVA-analysis, p=0.0005; Dunnett's test for multiple comparison, DMSO vs. probe: p=0.0032, probe vs. comp.: p= 0.0004, n=4, data are means ± SD). B) In silico docking analysis C) Platelet adhesion on collagen-coated flow chamber comparing control, ASA-treatment and ASA- and EPA-treatment (paired t-tests, control vs. ASA, p=0.0064, ASA vs. ASA + EPA, p>0.05, data are means ± SD) (D) The bar plot shows AA-induced maximum of aggregation in control, ASA- and ASA + EPA-treated human platelets.(paired t-tests, p>0.05, n=4, data are means ± SD).

E) The bar plot shows AA-induced maximum of aggregation with different concentration of AA in control and ASA- and EPA-treated human platelets. (EPA-treated platelets on the right: ANOVA-analysis, p=0.0313; Dunnetts' test for multiple comparison, 0.5mM vs. 1mM: p=0.0111, 0.5 mM vs. 2 mM: p=0.0397, n=7, data are means ± SD; ASA-treated platelets in the middle, ANOVA-analysis, p>0.05, n=7, data are means ± SD). F) Correlation of AA-induced maximum of aggregation (MoA) and plasma triglyceride concentrations (Pearson-correlation, n=370, p=0.6235, R^2= 0.0006556, r=0.02560). G) The bar plots show delta of t10-t0 AA/EPA ratio during ex-vivo platelet activation (unpaired t-test, p>0.05, n=27, data are means ± SD). H) Heat map of 20:4 and 20:5 containing lipids showing the comparison between before and after ten days of IPE-supplementation. Scale bar indicates fold change in comparison to control. Relative changes in AA stimulated samples vs control are shown for t0 (before intake) and t10 (10 days of treatment). I) Relative COX-1 inhibition is shown in dependency of EPA-concentrations (n=3, data are means ± SD).

Figure 5: Pharmacological inhibition of platelet COX-1 and genetic deficiency of platelet COX-1 abolished the antiplatelet effects of IPE-supplementation in vivo.

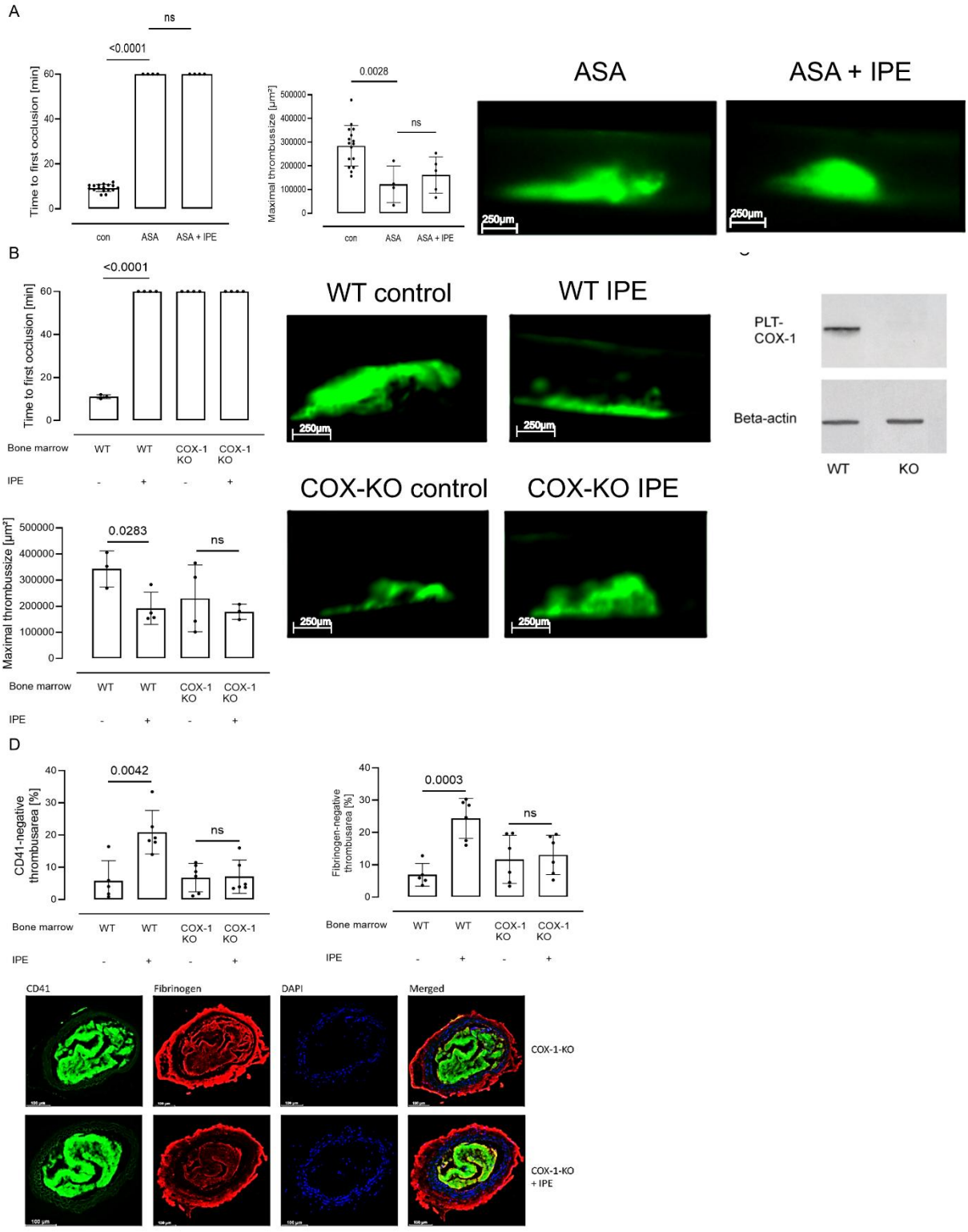

A) The bar plots show time to first occlusion in a carotid injury model of arterial thrombosis comparing ASA-treated and EPA+ASA-treated mice (left bar plot, unpaired t-test, $p>0.05$, n=4, data are means ± SD) and (and maximal thrombus size (right bar plot, unpaired t-test, $p>0.05$, $n_{control}=16$, $n_{ASA}=4$, $n_{ASA+IPE}=5$, data are means ± SD). Representative images are shown on the right with green fluorescence indicating thrombus in the carotid artery (left image, ASA, right image, ASA + IPE). B) The bar plots show time to first occlusion (upper bar plot, wildtype: control vs. IPE, unpaired t-test, $p<0.0001$, n=4, data are means ± SD; COX-1-deficiency: control vs. IPE, unpaired t-test, $p>0.05$, n=4, data are means ± SD) and thrombus size (lower

bar plot, wildtype: control vs. IPE, unpaired t-test, p=0.0283, n=4, data are means ± SD; COX-1-deficiency: control vs. IPE, unpaired t-test, p>0.05, n=4, data are means ± SD Representative images of intravital thrombus formation are shown on the right (upper left: wildtype control, upper right: wildtype IPE-treatment, lower left: COX-KO control, lower right: COX-KO IPE-treatment, green fluorescence indicates thrombus in the carotid artery). C) Representative western blot for platelet COX-1 in wildtype and platelet C*ox-1* deficient mice. D) The bar plots show CD41-negative thrombus area (left, wildtype: control vs. IPE, unpaired t-test, p=0.0042, $n_{control}$=5, n_{IPE}=6, data are means ± SD, COX-1-deficiency: control vs. IPE, unpaired t-test, p>0.05, n=6, data are means ± SD) and fibrinogen-negative thrombus area (right, wildtype: control vs. IPE, unpaired t-test, p=0.0003, $n_{control}$=5, n_{IPE}=6, data are means ± SD; COX-1-deficiency: control vs. IPE, unpaired t-test, p>0.05, n=6, data are means ± SD). Representative histological images (below) show CD41 in green, fibrinogen in red, and DAPI stained nuclei in blue. Control is shown in the upper line and IPE-treatment is shown below. Scale bars are given for 100µM.

Figure 6: IPE reduced platelet adhesion, aggregation, and degranulation ex vivo. Change from IPE treatment to EPA/DHA treatment abolished this effect.

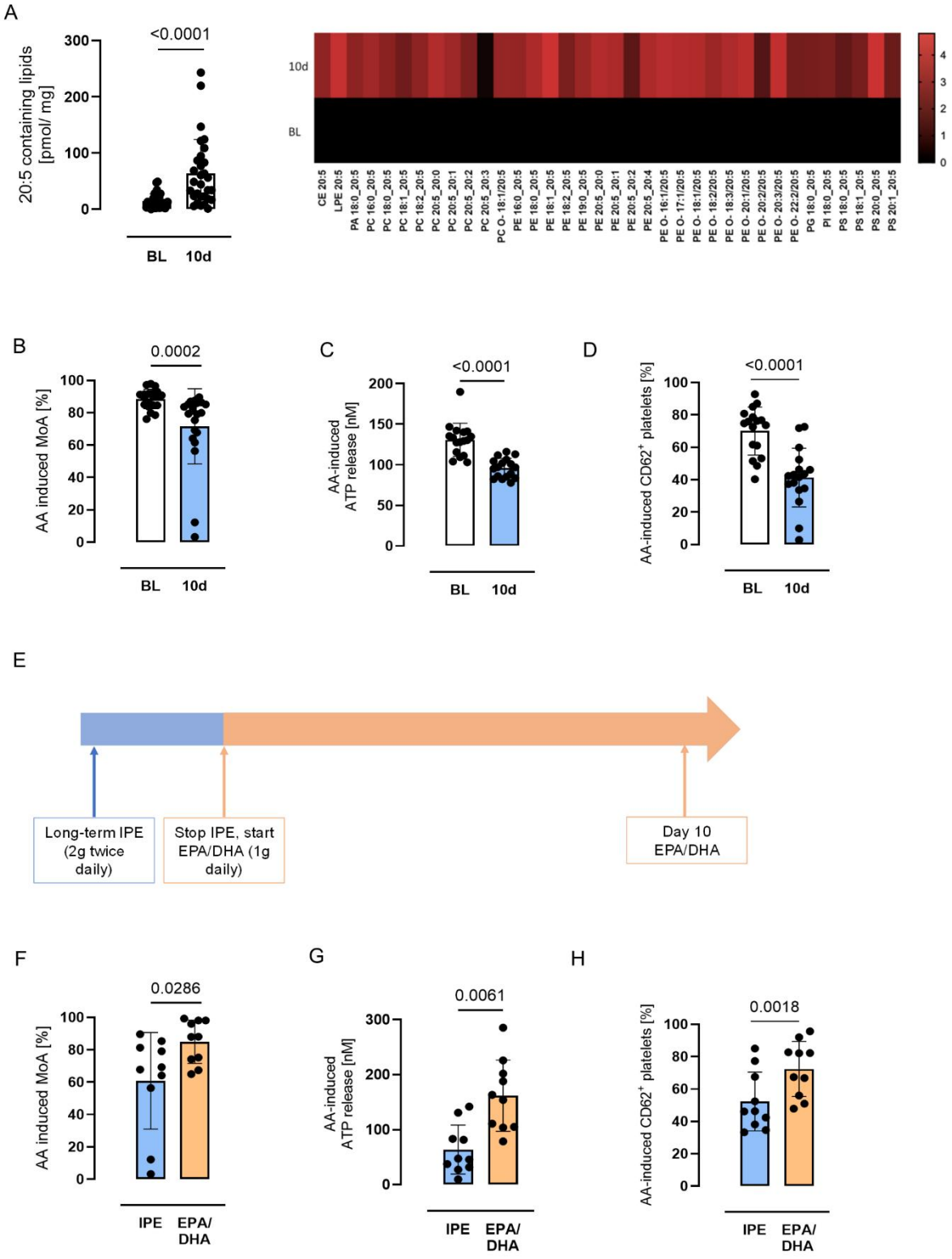

A) The bar plots show amount of 20:5 containing lipids after ten days of IPE-supplementation (left, Wilcoxon-test, p<0.0001, n=29, data are means ± SD). Heat map (right) showing the change of 20:5 containing lipids in the platelet membrane after 10 days. Scale bar indicates fold change from baseline to day ten. B) The bar plot shows AA-induced platelet aggregation (Wilcoxon-test, p=0.0002, n=20, data are means ± SD). C) The bar plot shows AA-induced adenosine-triphosphate (ATP)-release from platelets (paired t-test, p<0.0001, n=17, data are means ± SD). D) The bar plot shows AA-induced p-selectin expression on platelets (paired t-

test, p<0.0001, n=17, data are means ± SD). E) Blood was conducted from patients on long-term IPE medication and ten days after switching to an EPA-DHA-combi preparation. F) The bar plot shows AA-induced platelet aggregation before and after ten days of switching from EPA to EPA/DHA (paired t-test, p=0.0286, n=10 data are means ± SD). G) The bar plot shows AA-induced ATP-release before and ten days after switching from IPE to EPA/DHA-medication (paired t-test, p=0.0061, n=10, data are means ± SD). H) The bar plot shows AA-induced p-selectin expression before and ten days after switching from IPE to EPA/DHA-medication (paired t-test, p=0.0018, n=10, data are means ± SD).